

# Intrinsic susceptibility and bond defects in the novel 2D frustrated antiferromagnet $\text{Ba}_2\text{Sn}_2\text{ZnCr}_{7p}\text{Ga}_{10-7p}\text{O}_{22}$

D. Bono,<sup>1</sup> P. Mendels,<sup>1</sup> G. Collin,<sup>2</sup> and N. Blanchard<sup>1</sup>

<sup>1</sup>*Laboratoire de Physique des Solides, UMR 8502, Université Paris-Sud, 91405 Orsay, France*

<sup>2</sup>*Laboratoire Léon Brillouin, CE Saclay, CEA-CNRS, 91191 Gif-sur-Yvette, France*

(Dated: May 22, 2019)

We present microscopic and macroscopic magnetic properties of the highly frustrated antiferromagnet  $\text{Ba}_2\text{Sn}_2\text{ZnCr}_{7p}\text{Ga}_{10-7p}\text{O}_{22}$ , respectively probed with NMR and SQUID experiments. The  $T$ -variation of the intrinsic susceptibility of the  $\text{Cr}^{3+}$  frustrated kagomé bilayer,  $\chi_{kag}$ , displays a maximum around 45 K. The dilution of the magnetic lattice has been studied in detail for  $0.29 \leq p \leq 0.97$ . Novel dilution independent defects, likely related with magnetic bond disorder, are evidenced and discussed. We compare our results to  $\text{SrCr}_{9p}\text{Ga}_{12-9p}\text{O}_{19}$ . Both bond defects and spin vacancies do not affect the average susceptibility of the kagomé bilayers.

PACS numbers: 75.30.Cr, 75.50.Lk, 76.60.-k

Geometric frustration in antiferromagnets has proven to yield various original ground states in the past decade, from fluctuating  $T = 0$  ones, called generically “spin liquids”, to exotic freezings as spin ice. Most of these systems have in common a simple Heisenberg Hamiltonian with near neighbour ( $nn$ ) interactions on a corner sharing lattice. The diversity in this family is due to small deviations from the pure Heisenberg case, such as disorder, anisotropy, or weak additional interactions [1] which, in a classical picture, lift the frustration-induced macroscopic degeneracy of the ground state.

So far, there is no ideal experimental candidate for a spin liquid behavior, but a few, like the newly discovered  $\text{Ba}_2\text{Sn}_2\text{ZnCr}_{7p}\text{Ga}_{10-7p}\text{O}_{22}$  compound (BSZCGO( $p$ )) [2], retain the essence of the expected features, *e.g.* a short correlation length  $\xi$  [3] which prevents the occurrence of any long range order in a broad  $T$ -range below the Curie-Weiss (CW) temperature  $\theta_{CW}$ , a large residual entropy [2], and persistent fluctuations at  $T \rightarrow 0$  [4]. The corner sharing magnetic lattice of BSZCGO( $p$ ) is made of well decoupled  $\text{Cr}^{3+}$  ( $S = \frac{3}{2}$ ) 2D kagomé bilayers *only*. Interestingly, the  $nn$  direct couplings between  $\text{Cr}^{3+}$  ions make the Hamiltonian quite close to the ideal Heisenberg case [5]. A spin-glass like transition occurs at  $T_g \approx 1.5$  K [2], well below  $\theta_{CW} \approx 350$  K, which yields the highest *frustration ratio*  $f = \theta_{CW}/T_g \sim 230$  reported so far in a compound where frustration is driven by corner sharing equilateral triangles [6].

In comparison, the long-studied parent  $\text{Cr}^{3+}$  compound  $\text{SrCr}_{9p}\text{Ga}_{12-9p}\text{O}_{19}$  (SCGO( $p$ )) [7] ( $f \sim 150$ ) is not made of frustrated bonds only, since  $\frac{2}{9}$  of the  $\text{Cr}^{3+}$  form pairs which separate the bilayers and couple into singlets below 216 K [8].  $\text{Ga}^{3+}/\text{Cr}^{3+}$  substitutions of the order of a few percent ( $\sim 1 - p$ ) represent the major drawback in SCGO( $p$ ) since they introduce paramagnetic centers in between the bilayers by breaking these  $\text{Cr}^{3+}$  pairs. This not well-controlled parameter, together with the shorter inter-bilayer distance, 6.4 Å instead of 9.4 Å in BSZCGO( $p$ ) [2, 8], is likely to make the physics of

SCGO( $p$ ) less 2D and complicates the search for the intrinsic kagomé physics.

We present the first NMR study of BSZCGO( $p$ ) and show that the intrinsic susceptibility ( $\chi_{kag}$ ) displays a maximum at a temperature comparable to the  $nn$  Heisenberg coupling  $J$ . The similarity of the  $T$ -variation of  $\chi_{kag}$  with the case of SCGO( $p$ ) stresses the universal character of this maximum in  $\chi_{kag}$  for kagomé bilayers. As a *local* probe, Ga NMR, contrary to SQUID, offers a unique way to disentangle  $\chi_{kag}$  from the contribution of “magnetic defects” to macroscopic susceptibility [5, 9]. This gives evidence for two types of defects, for  $0.29 \leq p \leq 0.97$ , (*i*) the spin vacancies due to the  $\text{Ga}^{3+}/\text{Cr}^{3+}$  substitution which was shown to generate a staggered response of the surrounding magnetic background [5] and (*ii*) novel dilution independent defects, discussed here.

All the samples were synthesized by a solid state reaction of  $\text{BaCO}_3$ ,  $\text{Cr}_2\text{O}_3$ ,  $\text{Ga}_2\text{O}_3$ ,  $\text{ZnO}$  and  $\text{SnO}_2$  in air at 1400°C. They were characterized by X-ray diffraction, macroscopic susceptibility ( $\chi_{macro}$ ) measurements and  $^{71}\text{Ga}$  NMR. The synthesis of pure samples with  $p > 0.97$  failed. Indeed, in this case, X-ray diffraction shows a  $\text{Cr}_2\text{O}_3$  parasitical phase and an extra kink of  $\chi_{macro}$  is also observed around 6 K. This sets the maximum of the  $\text{Cr}^{3+}$  lattice occupancy to a value of  $p_{max} = 0.97$ . Below  $p_{max}$ , Ga substitutes randomly on the Cr(1a, 6i) site.

The two  $\text{Ga}^{3+}$  site environments ( $p = 1$ ), are displayed in the inset of Fig. 1(b). The Ga(2d) site is coupled to 3p Cr(1a) and 9p Cr(6i) through neighbouring oxygens. Its local charge environment is approximately cubic, whereas the Ga(2c) site belongs to a tetrahedron elongated along the  $c$ -axis and couples to 3p Cr(6i).

We performed  $^{71}\text{Ga}$  sweep field NMR experiments at constant frequency  $\nu_l = 84.365$  MHz, using a  $\frac{\pi}{2}-\tau-\pi$  spin echo sequence. Two sites can be clearly identified in Fig. 1 with the expected ratio of integrated intensities close to 2:1. At 150 K, the double peak around the reference field  $H_l \approx 6.498$  T in Fig 1(a) is characteristic of a 0.53% slightly shifted  $\frac{1}{2} \leftrightarrow -\frac{1}{2}$  nuclear transition, with

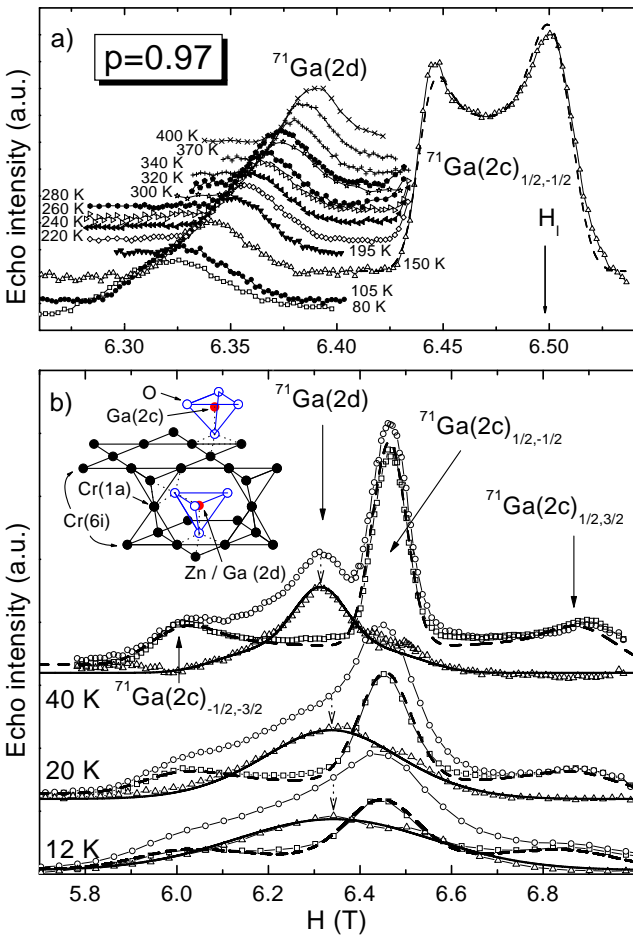


FIG. 1:  $^{71}\text{Ga}$  spectra. a)  $T \geq 80$  K. The  $^{71}\text{Ga}(2c)$  first order quadrupolar contribution appears as a flat background in this field range. b)  $T \leq 40$  K, lines are broadened.  $\circ$  and  $\square$  are the short  $\tau$  and the rescaled long  $\tau$  spectra respectively.  $\triangle$  is for the  $^{71}\text{Ga}(2d)$  contribution, given by their subtraction. The dotted arrows point the center of the  $^{71}\text{Ga}(2d)$  line. Continuous (dashed) lines are gaussian broadened  $^{71}\text{Ga}(2d)$  ( $^{71}\text{Ga}(2c)$ ) powder pattern quadrupolar simulation, with  $\nu_Q = 3.5$  MHz (12.3 MHz) and  $\eta = 0.6$  ( $\eta = 0.14$ ). Inset :  $\text{Ga}^{3+}$  sites.

second order quadrupolar powder pattern. The corresponding first order satellite singularities are clearly seen in the less expanded spectra of Fig. 1(b). From these singularities, we extract a quadrupolar frequency  $^{71}\nu_Q \approx 12.3$  MHz and an asymmetry parameter  $\eta = 0.14(2)$  [10]. The other line is more shifted  $\sim 2\%$  (Fig. 1(a)). Its shape can be explained by a quite broadened  $S = \frac{3}{2}$  quadrupolar pattern, with  $^{71}\nu_Q = 3.5 \pm 1$  MHz (Fig. 1(b)) [19]. The intensity ratio, the very different quadrupolar frequency associated with different charge environment, and the analogy with SCGO allow us to identify unambiguously the  $^{71}\text{Ga}(2c)$  and  $^{71}\text{Ga}(2d)$  sites. Though, contrary to SCGO( $p$ ), we could not identify any line typical of Ga substituted site.

At low- $T$ , the two lines are found to overlap due to strong broadenings. In order to deconvolute the two con-

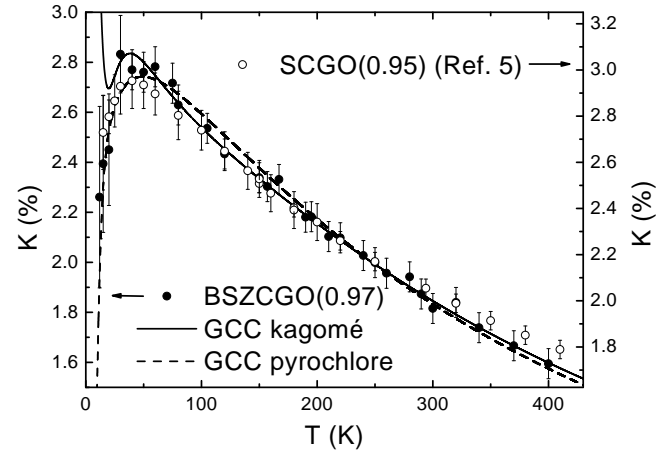


FIG. 2: Shift of the  $^{71}\text{Ga}(2d)$  ( $\text{Ga}(4f)$ ) line for BSZCGO (SCGO, from Ref. 5). The lines are fits described in the text. The error bars on  $K_{2d}^{71}$  are enhanced at lower temperatures because of the strong broadening of the line.

tributions, we took advantage of the different transverse relaxation times  $T_2$  of the two lines (Fig. 1b). The first step was to use a large  $\tau$  spectrum ( $\tau = 200 \mu\text{s}$ ) to isolate the  $^{71}\text{Ga}(2c)$  contribution ( $T_{2,2c}^{71} \approx 200 \mu\text{s}$ ). Its linewidth  $\Delta H$  is extracted using a gaussian convolution of the high- $T$  quadrupolar pattern. In the second step, we used the short  $\tau$  spectrum ( $\tau \approx 10 \mu\text{s}$ ) where the  $^{71}\text{Ga}(2d)$  contribution is evident, and subtracted the  $T_{2,2d}^{71}$  normalized long  $\tau$  spectrum. The width and the shift of the  $^{71}\text{Ga}(2d)$  line can then be extracted from a fit using a  $^{71}\nu_Q = 3.5$  MHz quadrupolar pattern convoluted by a gaussian line shape, not affected by the 30% uncertainty on  $^{71}\nu_Q$ . As a matter of consistency, the ratio  $I_{2c}^{71}/I_{2d}^{71} = 2 \pm 0.8$  stays close to 2/1 down to 10 K. No significant loss of intensity was observed down to this temperature.

The kagomé bilayer susceptibility  $\chi_{kag}$  is revealed in the shift  $K_{2d}^{71}$  of the  $^{71}\text{Ga}(2d)$  line [9], presented in Fig. 2. It increases when  $T$  decreases for  $T \geq 80$  K, reaches a maximum around  $T_{max} \approx 45$  K and decreases below. A phenomenological CW law,  $K_{2d}^{71} = C_{NMR}/(T + \theta_{NMR})$ , is an accurate fit for  $T > 80$  K with  $\theta_{NMR} = 380 \pm 10$  K. Although very common, this is a rather crude approximation in a  $T$ -range lower than  $\theta_{NMR}$ . Using high- $T$  series expansion of the susceptibility for a pure kagomé lattice, the true CW temperature  $\theta_{CW}$  can be deduced by correcting  $\theta_{NMR}$  by a factor 1.5 [11]. From  $\theta_{CW} = zS(S+1)J/3$  and  $z = 5.14$  the average number of  $nn$  for the  $\text{Cr}^{3+}$  of the bilayer, we extract  $J \approx 40$  K.

In SCGO(0.95) [5], a value  $\theta_{NMR} = 440 \pm 5$  K [20], was found and  $C_{NMR}$  is 20% larger. The small variation in the CW behaviours can be explained by a slightly larger  $\text{Cr}^{3+}\text{-Cr}^{3+}$  coupling, due to a 0.01 Å mean shorter bond, and  $\Delta J/\Delta d \sim 450$  K/Å [5].

The existence of a gap in  $\chi_{kag}$  was already an important issue for SCGO(0.89) in Ref. 9. Rather than a gap,

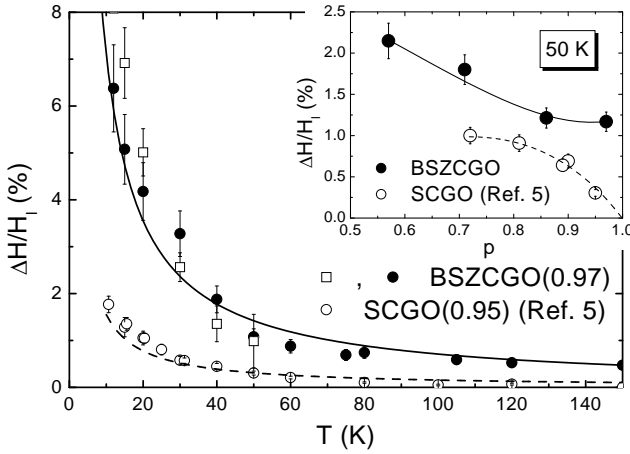


FIG. 3: Magnetic contribution to the NMR linewidth  $\Delta H/H_l(^{71}\text{Ga}(2\text{d}))$  ( $\bullet$ ). Data for the  $^{71}\text{Ga}(2\text{c})$  ( $\square$ ) are also presented rescaled by a factor 6, corresponding to the ratio of hyperfine coupling constants consistent with the high- $T$  shifts. The lines are  $\propto 1/T$  fits. Inset :  $p$ -dependence of  $\Delta H_2^{71}$  ( $\Delta H_4^{71}$ ) at 50 K for BSZCGO( $p$ ) (SCGO( $p$ )). The lines are guides to the eye.

it was suggested that the maximum of  $\chi_{kag}$  would be a landmark of the moderate increase of magnetic correlations. This was later confirmed by neutron measurements [12], and further studied theoretically using the “generalized constant-coupling” (GCC) method [13]. The starting point is a  $nn$  Heisenberg hamiltonian with the assumption of short range magnetic correlations if some, as proven experimentally [14]. The thermodynamical susceptibility of *one spin unit*, made of triangles (kagomé) or tetrahedras (pyrochlore), is first calculated in the presence of an external field. The susceptibility of *one spin* is then expressed in a mean field approach of the coupling with the two units it belongs to. Finally, the spin susceptibility is computed with a self consistent equation. The fits for  $S = \frac{3}{2}$  kagomé and pyrochlore models, in between which the kagomé bilayer susceptibility is expected to lie, yield very close values of the CW temperature  $\theta_{CW} = 238 \pm 3$  K (Fig. 2). One extracts  $J \approx 37$  K for BSZCGO(0.97), consistent with the high- $T$  series expansion.

Beyond expectation, the GCC computation fits quite well the data even below  $T_{max}$ . This in turn indicates that the strongest underlying assumption of this model is relevant, *i.e.* that  $\xi$  is of the order of the lattice parameter.

The linewidth is the second important piece of information which we extract from our data. It is indeed due to a distribution of susceptibility which is related to the existence of defects and to their nature [5]. In Fig. 3, we compare the linewidth  $\Delta H/H_l$  obtained for BSZCGO(0.97) to the one obtained for a comparable dilution in SCGO(0.95). In both samples,  $\Delta H/H_l$  fol-

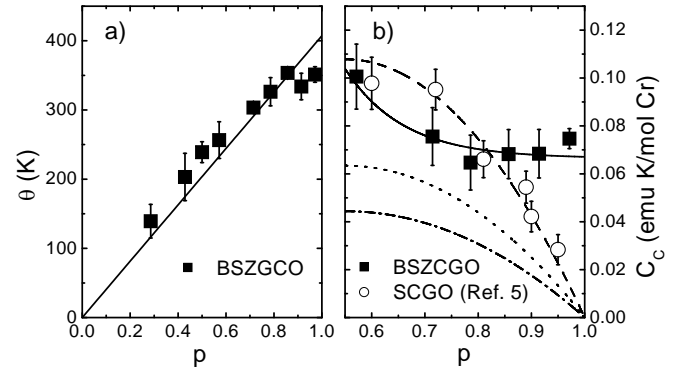


FIG. 4: Results of the fits of SQUID data (Eq. 1). a)  $\theta(p)$  with linear fit. b)  $C_C(p)$ , continuous and dashed lines are guides to the eye. Dotted and dash-dotted lines are a sketch of the two contributions to  $\chi_{macro}$  from the Ga/Cr substitutions, respectively in the kagomé bilayers and in the dimers sites in SCGO( $p$ ).

lows a Curie-like behaviour which has been shown to be characteristic of magnetic defects in SCGO( $p$ ). Surprisingly, in BSZCGO(0.97), the linewidth is *4 times larger* than in SCGO(0.95). This ratio cannot be explained by a variation of hyperfine constant, which, from the ratios of  $C_{NMR}$ , was estimated to a maximum of 20%. In addition, the Ga(2d) linewidth in BSZCGO( $p$ ) could be measured for various  $p$  at  $T = 50$  K (Fig. 3(inset)). Contrary to the case of SCGO( $p$ ), where  $\Delta H/H_l$  extrapolates to 0 for a perfect lattice ( $p = 1$ ), we find that it reaches an asymptotic non-zero value in BSZCGO( $p$ ) for  $0.86 \leq p < 1$ . One could wonder whether the dilution of the magnetic lattice could be larger than the nominal one. This can be ruled out since (i) we found the expected evolution of the lineshape at 300 K with  $p$  [15] (ii) muon spin relaxation measurements indicate a regular evolution of the dynamical properties with  $p$  [4]. We then conclude that the extra width is not related to spin vacancies and reflects new  $p$ -independent defects in BSZCGO( $p$ ).

Defect terms could also be probed using low- $T$  macroscopic susceptibility measurements. Using a commercial SQUID magnetometer, we performed magnetization measurements under a field of 100 G, for  $0.29 \leq p \leq 0.97$ , down to 1.8 K. No difference has been observed between Field Cooled and Zero Field Cooled branches down to this temperature, in agreement with Ref. 2. Along the common route, one can simply analyze the data using the phenomenological fit :

$$\chi_{macro}(p) = \frac{C_{CW}(p)}{T + \theta(p)} + \frac{C_C(p)}{T + \theta_C(p)}. \quad (1)$$

The first term reflects the high- $T$  weak variation of the susceptibility due to AF interactions. From this fit, we can extract a  $p$ -independent effective moment per  $\text{Cr}^{3+}$ ,  $p_{eff} = 4.1 \pm 0.2/\mu_B$ , close to  $3.87/\mu_B$  expected for  $S = \frac{3}{2}$ .

From the linear variation of  $\theta(p) \approx 1.5\theta_{CW}(p)$  (Fig. 4(a)), we extract  $J \sim 40$  K, consistent with our NMR result.

The second term in Eq. 1 is introduced to fit the low- $T$  behaviour associated with the defects [5, 16]. It is close to purely Curie law, with  $\langle \theta_C(p) \rangle = 1 \pm 0.5$  K. Values of the Curie constants  $C_C$  are reported in Fig. 4(b). We find a  $p$ -dependence qualitatively similar to the NMR width data, *i.e.* a finite flat variation for  $BSZCGO(p \rightarrow 1)$ . To give an order of magnitude, this term represents 20% of  $S = \frac{1}{2}$  paramagnetic spins with respect to the number of  $Cr^{3+}$  spins. Once the dilution defect term becomes significant ( $p \leq 0.8$ ), the  $C_C(p)$  slope is qualitatively comparable in both samples.

One can notice that there is a crossing between the variation of  $C_C(p)$  of the two compounds (Fig. 4(b)) which is not observed in the NMR width  $\Delta H$  (Fig. 3(insert)). Since in  $\chi_{macro}$  all contributions add, we tentatively attribute this difference to the substituted  $Cr^{3+}$  pairs in  $SCGO(p)$ , not probed by Ga NMR. In order to estimate their contribution to  $\chi_{macro}$ , we determine first the scaling ratio between  $\Delta H$  and  $\chi_{macro}$  in  $BSZCGO(p)$ , where only kagomé bilayers are present. We then assume that the relationship between defects and width is the same in  $SCGO(p)$  and deduce from the NMR width in  $SCGO$  the contribution of defects in the bilayer to  $\chi_{macro}$ . Hence, the difference with  $\chi_{macro}(SCGO)$  comes from the  $Cr^{3+}$  pairs sites which is found sub-stoichiometric, in agreement with Ref. 5.

To summarize, low- $T$  macroscopic susceptibility and NMR width data can be both satisfactorily accounted for, only if a novel  $p$ -independent defect-like contribution is taken into consideration, a result somehow surprising in view of the close similarity between kagomé bilayers. We now elaborate about the nature of these defects. The only major change lies in the 1:1 random occupancy of the 2d site by  $Ga^{3+}$  or  $Zn^{2+}$  ions which induces different electrostatic interactions with the neighbouring ions. As an example, distances to oxygens in a tetrahedral environment vary from  $r_{Ga^{3+}-O^{2-}} = 0.47$  Å to  $r_{Zn^{2+}-O^{2-}} = 0.60$  Å which is at the origin of a change of the average  $Ga(4f,2d)$ -O bonds, from 1.871 Å for  $SCGO$  to 1.925 Å in  $BSZCGO$  [2, 8]. Similarly, one expects that the  $Cr^{3+}$  ions will be less repelled by  $Zn^{2+}$  than by  $Ga^{3+}$ . This will certainly induce magnetic bond-disorder, *i.e.* a modulation of exchange interactions  $J$  between neighbouring  $Cr^{3+}$ . As seen before, one can estimate that a modulation as low as  $\sim 0.01$  Å in the  $Cr^{3+}$ - $Cr^{3+}$  distances would yield a 10% modulation of  $J$ .

The presence of non-perfect equilateral triangles classically induces a paramagnetic component in the susceptibility of the frustrated units [17]. The fact that we do not observe any extra Curie variation as compared to  $SCGO(p)$  in the average susceptibility, probed through the NMR shift  $K_{2d}^{71}$  (Fig. 2), indicates that such unbalanced exchange interactions only induce a staggered response in the same manner as spin vacancies [5]. Whether

this could be connected with localization of singlets in the vicinity of defects [18] and a staggered cloud around should be more deeply explored. This might highlight the relevance of a RVB singlet approach to the physics of the kagomé network. Further insight into the exact nature of the defects likely require a better determination of the bond disorder through structural studies at low- $T$ , to avoid the usual thermal fluctuations at room  $T$ .

To conclude, one of our major findings is the maximum of the local susceptibility  $\chi_{kag}$  observed around 45 K for *both*  $BSZCGO(p)$  and  $SCGO(p)$ , which appears very robust to the presence of defects either spin vacancies as observed in Ref. 5 or bond disorder as pointed out above. This intrinsic susceptibility is very close to theoretical model of  $S = \frac{3}{2}$  kagomé or pyrochlore with correlation length of the order of magnitude of the  $Cr^{3+}$ - $Cr^{3+}$  bond. Finally, we showed that bond disorder is likely to give raise, like spin vacancies, to extended defects which underline the correlated nature of the kagomé network. This study of “impurities” might be a major avenue for revealing the nature of the ground state in a similar manner as in low-D quantum magnetism studies.

- 
- [1] A. Chubukov, Phys. Rev. Lett. **69**, 832 (1992); R. Moessner, Phys. Rev. B **57**, R5587 (1998); S.E. Palmer and J.T. Chalker, Phys. Rev. B **62**, 488 (2000); M. Elhajal, B. Canals, and C. Lacroix, Phys. Rev. B **66**, 014422 (2002).
  - [2] I.S. Hagemann *et al.*, Phys. Rev. Lett. **86**, 894 (2001).
  - [3] P. Bonnet *et al.*, to be published in Highly Frustrated Magnets 2003 conference proceedings, J. Phys. Cond. Mat.
  - [4] D. Bono *et al.*, in preparation.
  - [5] L. Limot *et al.*, Phys. Rev. B **65**, 144447 (2002).
  - [6] A.P. Ramirez, Annu. Rev. Mater. Sci. **24**, 453 (1994).
  - [7] X. Obradors *et al.*, Solid State Commun. **65**, 189 (1988).
  - [8] S.-H. Lee *et al.*, Phys. Rev. Lett. **76**, 4424 (1996).
  - [9] P. Mendels *et al.*, Phys. Rev. Lett. **85**, 3496 (2000).
  - [10] A. Keren *et al.*, Phys. Rev. B **57**, 10745 (1998).
  - [11] A.B. Harris, C. Kallin, and A.J. Berlinsky, Phys. Rev. B **45**, 2899 (1992).
  - [12] C. Mondelli *et al.*, Physica B **267-268**, 139 (1999).
  - [13] A.J. García-Adeva and D.L. Huber, Phys. Rev. B **63**, 174433 (2001); Physica B **320**, 18 (2002).
  - [14] C. Broholm, G. Aeppli, G.P. Espinosa, and A.S. Cooper, Phys. Rev. Lett. **65**, 3173 (1990).
  - [15] D. Bono *et al.*, to be published in Highly Frustrated Magnets 2003 conference proceedings, J. Phys. Cond. Mat.
  - [16] P. Schiffer, and I. Daruka, Phys. Rev. B **56**, 13712 (1997).
  - [17] R. Moessner and A.J. Berlinsky, Phys. Rev. Lett. **83**, 3293 (1999).
  - [18] S. Dommange, M. Mambrini, B. Normand, and F. Mila, Phys. Rev. B **68**, 224416 (2003).
  - [19] Using a point charge computation, we could estimate a 30% distribution of  $\nu_Q$  and a very large distribution of  $\eta$  around 0.6, due to the  $Zn^{2+}/Ga^{3+}$  random occupation of the 2d site. It prevents the observation of any quadrupo-

- lar satellites at high- $T$ .
- [20] The difference in  $\theta_{NMR}$  with Ref. 5 comes from the chemical shift which was neglected there. We estimated it here to 0.15(3)% comparing  $K_{2d}^{71}$  and  $K_{2c}^{71}$  at high- $T$ .